



CNCS



# SUPRAMOLECULAR ORGANIC SEMICONDUCTING MATERIALS FOR OPTOELECTRONICS

Acronym: SUPRAMOL-MAT

Scientific Report STAGE 1/ 2022

Project code: PN-III-P4-PCE-2021-0906

PCE 120 din 14/06/2022

## PROJECT MANAGER

Dr. Aurica Farcaș

## TEAM MEMBERS

1. Dr. Ana-Maria Resmeriță
2. Dr. Ursu Laura-Elena
3. Dr. Balan-Porcărașu Mihaela
4. Dr. Asăndulesa Mihai
5. Dr. Tigoianu Ionuț Radu
6. Dr. Peptu Cristian

# ABSTRACT

The main objective of SUPRAMOL-MAT project is to adopt a systematic research process in order to generate successful results, owing to SMPs potential as next generation organic electronic materials.

We proposed in the first stage of the project the following two main objectives:

- O1.** The synthesis of a new family of host molecules
- O2.** The synthesis of new pseudopolyrotaxane and polyrotaxane architectures based on cucurbit[7]uril (CB7) and permodified  $\beta$ -cyclodextrin (host molecules) and 3,4-ethylenedioxythiophene (EDOT) guest molecules.

Three main directions were developed:

- a) synthesis of CB7 and of 2,3,6-tri-O-methyl  $\beta$ -cyclodextrin (TMe $\beta$ CD);
- b) synthesis of inclusion complexes or host-guest systems (EDOT·CB7) and (EDOT·TMe $\beta$ CD);
- c) synthesis of PEDOT·CB7 pseudopolyrotaxane and polyrotaxane architectures.

# O1 -The synthesis of a new family of host molecules

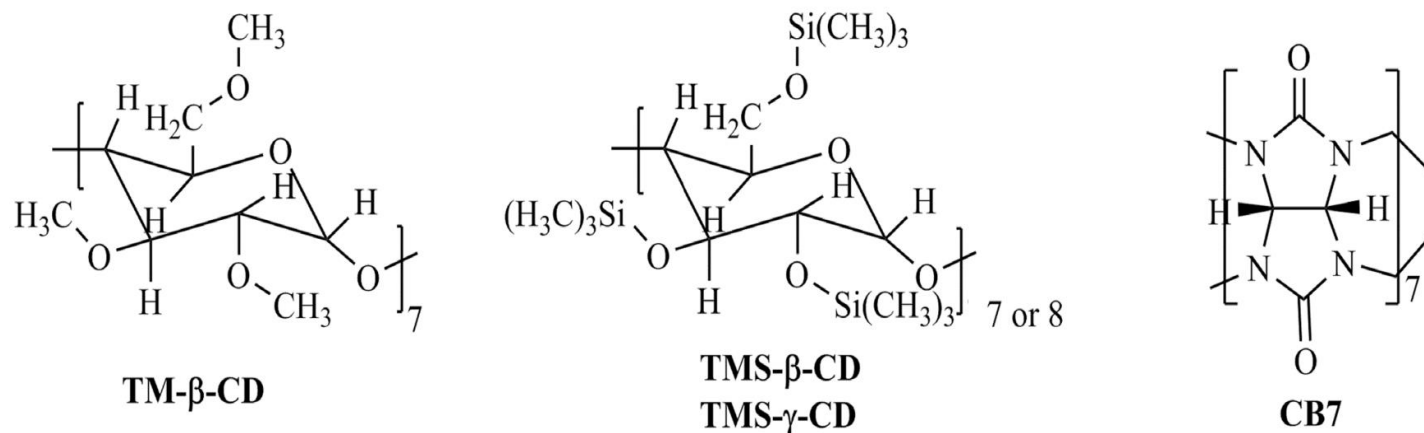


**Figure 1.** Chemical structures of host molecules.

## O.1.1 Synthesis of CB7

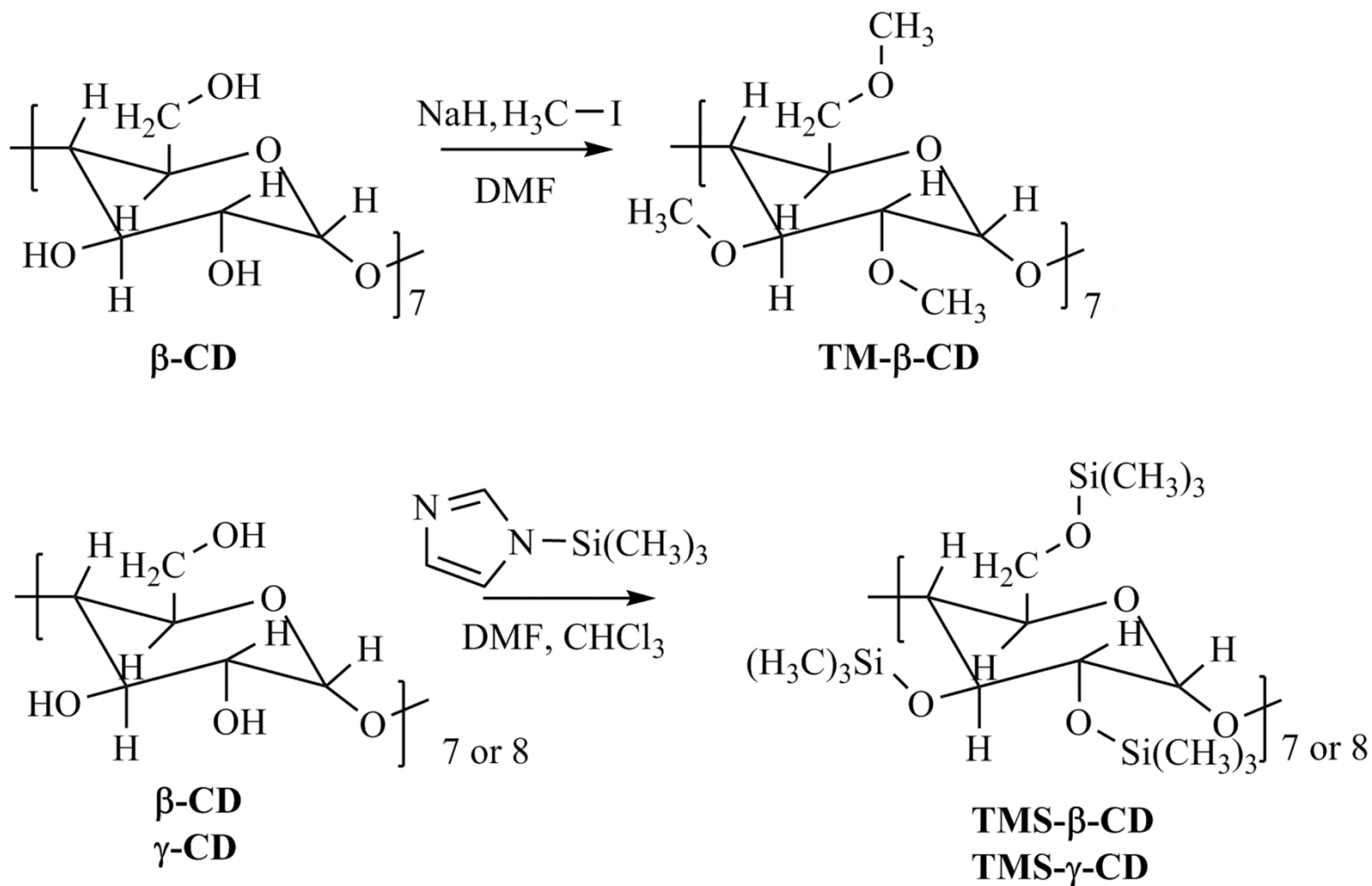
CB7 was obtained as a white solid powder. The chemical structure of CB7 was confirmed by FT-IR and  $^1\text{H}$  NMR spectroscopies.

FT-IR (KBr,  $\text{cm}^{-1}$ ): 3446 (N-H), 2926 (C-H), 1733 (C=O), 1476 (C-N), 1376, 1326, 1234, 1191, 967, 806, 760, 674, 626  $\text{cm}^{-1}$ .

$^1\text{H}$  NMR (DMSO- $d_6$ , ppm):  $\delta = 4.15$  (d, 14 H,  $J = 14.8$  Hz,  $\text{CH}_2$ ), 5.37 (s, 14 H, CH), 5.67 (d,  $J = 14.4$  Hz, 14 H,  $\text{CH}_2$ ).

$^1\text{H}$  NMR ( $\text{D}_2\text{O}$ , ppm):  $\delta = 4.25$  (d, 14 H,  $J = 15.2$  Hz,  $\text{CH}_2$ ), 5.55 (s, 14 H, CH), 5.80 (d,  $J = 15.6$  Hz, 14 H,  $\text{CH}_2$ ).

## O.1.2 Synthesis of chemically permodified cyclodextrins



**Scheme 1.** Synthesis of chemically permodified cyclodextrins.

# O2. The synthesis of poly(3,4-ethylenedioxythiophene) (PEDOT) /CB7 PPs and PRs architectures

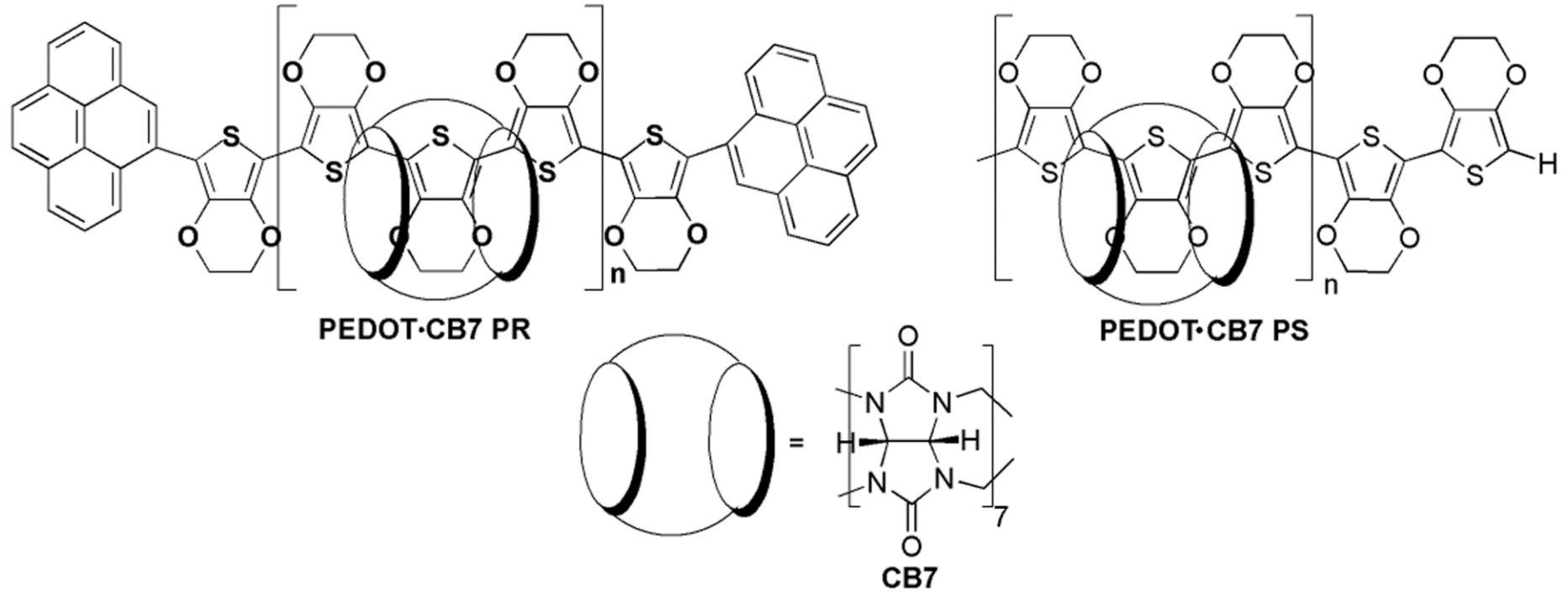


**Figure 2.** Chemical structures of PEDOT-CB7 PR and PEDOT-CB7 PS.

## Synthesis of EDOT·CB7 inclusion complexes

For this purpose, the EDOT was added to a CB7 solution in water in a molar ratio 1/1.5. The mixture was sonicated for 15 min and vigorously stirred at ambient temperature for 24 h under nitrogen ( $N_2$ ) to give a slurry mixture. After filtration, the solid was thoroughly washed with water and acetone to remove residual free CB7 and EDOT. After being dried, a white solid was obtained. The chemical structure of the EDOT·CB7 compound was verified by NMR spectroscopy. The  $^1H$  NMR analysis in  $DMSO-d_6$  confirmed the chemical structure of the EDOT·CB7 inclusion complex.

$^1H$  NMR ( $DMSO-d_6$ ),  $\delta$  (ppm): 6.56 (s, 2H, EDOT), 5.71 (d, 14 H,  $CH_2$  (CB7)), 5.33 (s, 14 H, CH (CB7)), 4.11 (s, 4H, EDOT), 4.07 (d, 14 H,  $CH_2$  (CB7)).

### Characterization data

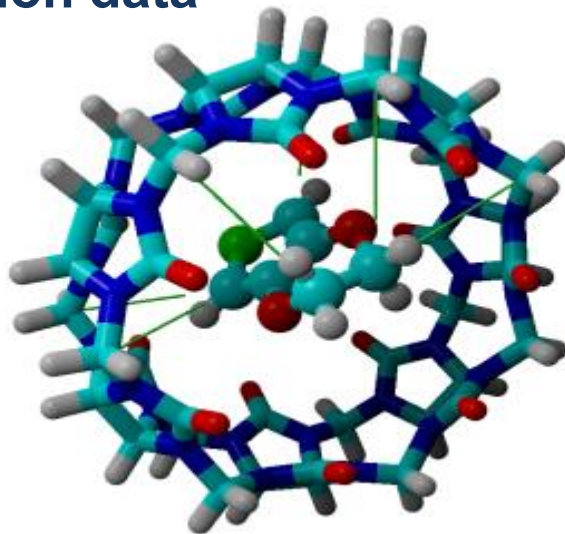


**Figure 3.** Molecular docking model of EDOT·CB7 inclusion complex formation and hydrophobic contacts illustrated as solid-green-lines.

## Synthesis of PEDOT·CB7-PPs

The EDOT·CB7 inclusion complex, which represented the starting monomer for the subsequent chemical oxidation reaction, was polymerized directly in water by the addition of a five-fold excess of FeCl<sub>3</sub> oxidant over the stoichiometric amount to the dispersion of EDOT·CB7 inclusion complexes. The mixture was sonicated for 15 min and vigorously stirred at ambient temperature for four days, in which a blue suspension was obtained. The solid was isolated by filtration, washed with acetone, methanol and water. After drying a dark-blue solid was obtained. Finally, the resulting solid was dispersed in water and vortex stirred for 20 min. The stable dispersion in water of PEDOT·CB7-PPs was transferred to a round bottom flask and dried by lyophilization.

<sup>1</sup>H-NMR (D<sub>2</sub>O), δ (ppm): 5.73 (d, 14 H CH<sub>2</sub>, (CB7)), 5.54 (s, 14 H, CH (CB7)), 4.47 (s, 4H, PEDOT), 4.26 (d, 14 H, CH<sub>2</sub> (CB7)).

<sup>1</sup>H-NMR (DMSO-d<sub>6</sub>), δ (ppm): 5.69 (d, 14 H, CH<sub>2</sub> (CB7)), 5.46 (s, 14 H, CH (CB7)), 4.53 (s, 4H, PEDOT), 4.18 (d, 14 H, CH<sub>2</sub> (CB7)).

FT-IR (KBr, cm<sup>-1</sup>): 3447, 2926, 1730, 1477, 1323, 1232, 1190, 966, 804, 756, 673 436 cm<sup>-1</sup>.

GPC (water with 0.02 % N<sub>3</sub>Na and 0.05 M LiBr as eluent, PEO standards):  $M_n \sim 9$  kDa,  $M_w/M_n \sim 2.6$ .

## Synthesis of PEDOT·CB7-PRs

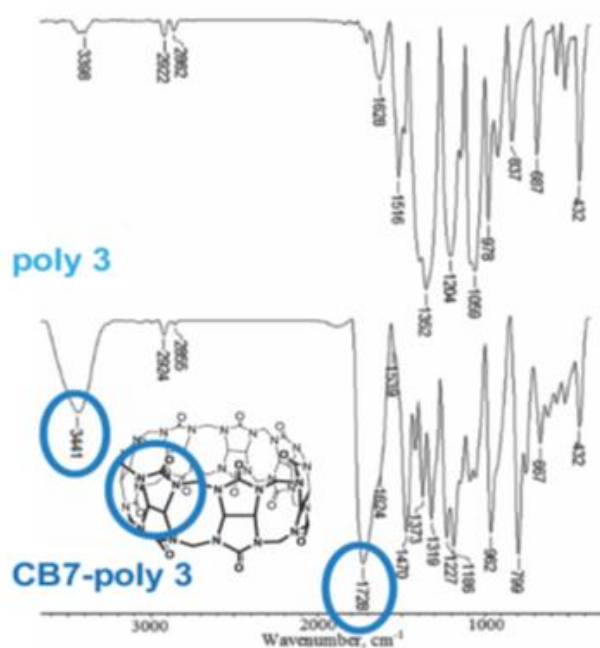
After the synthesis of PEDOT·CB7-PPs was completed, pyrene as stopper dissolved in DMF and small amount of  $\text{FeCl}_3$  as a fresh catalyst were added and the reaction was continued for 2 days. PEDOT·CB7-PRs was purified by a similar procedure that was used in the purification step of PEDOT·CB7-PPs. After drying, the PEDOT·CB7-PRs was obtained as a blue-dark solid.

$^1\text{H}$  NMR ( $\text{DMSO-d}_6$ ),  $\delta$  (ppm): 5.69 (d, 14H,  $\text{CH}_2$  (CB7)), 5.48 (s, 14H, CH (CB7)), 4.38 ( $\text{CH}_2$ , PEDOT overlapped with  $\text{CH}_2$  from CB7).

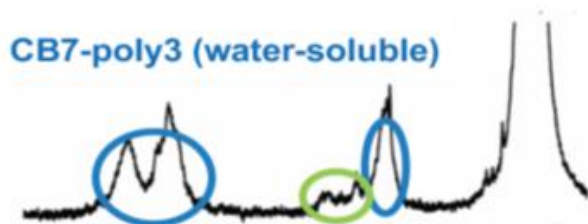


# Characterization of PEDOT-CB7 polyrotaxane

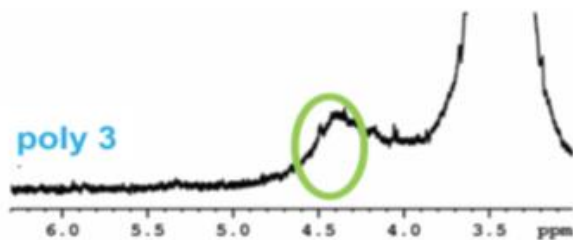
FT-IR



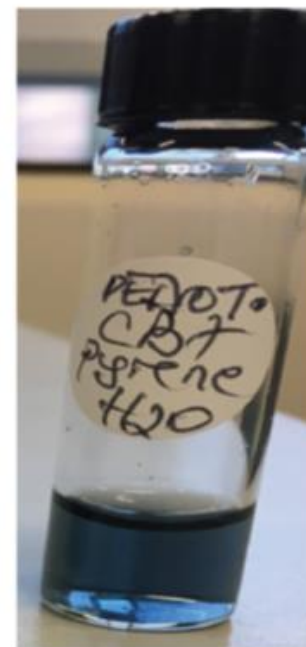
$^1\text{H}$  NMR in  $\text{DMSO-d}_6$



35-60% coverage ratio,  
compare cyclodextrin-polyrotaxanes <30%



Visual Color

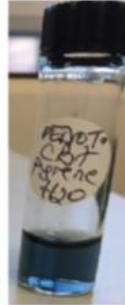


CB7-poly3

## Morphology

CB7-polymer has less flexible conformation.

## Solubility/Processability



CB7-poly3

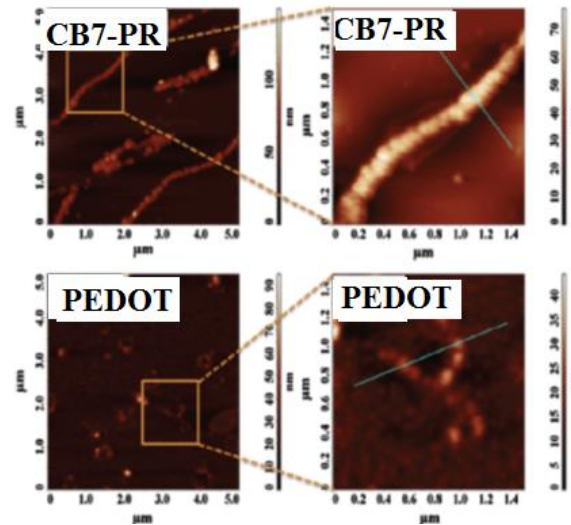


**Figure 4.** AFM images of PEDOT·CB7 PR and PEDOT thin films.

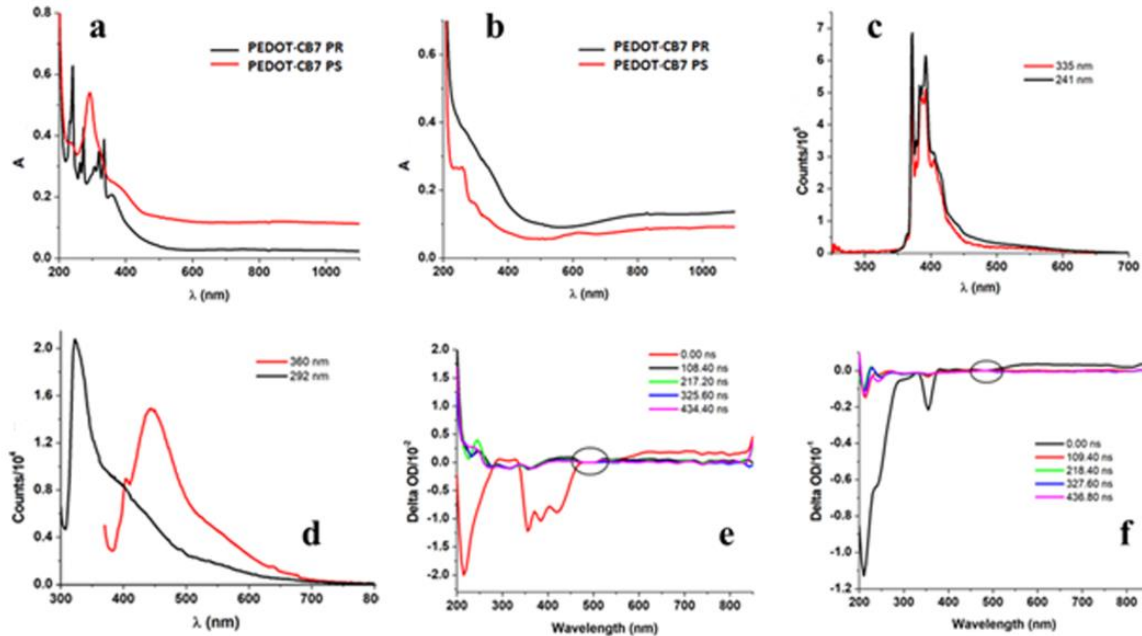
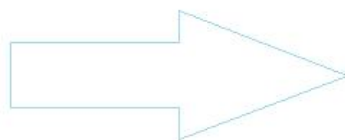
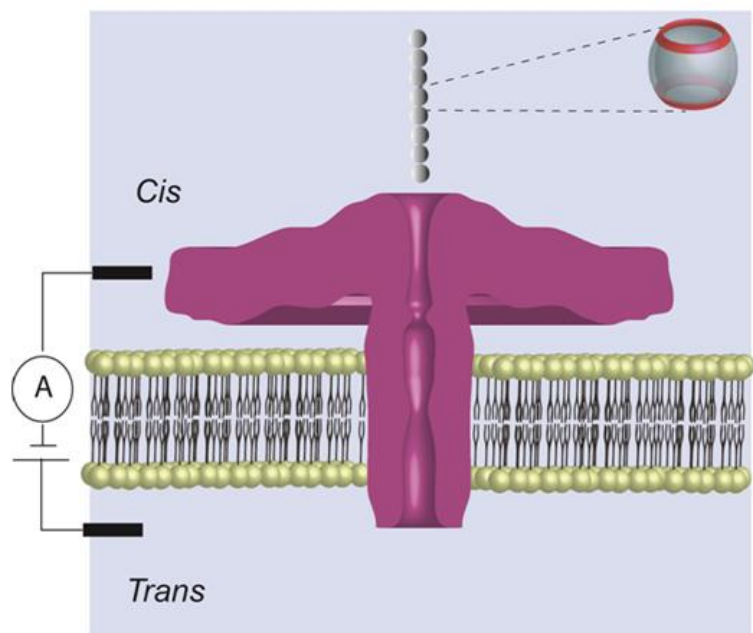


**Figure 5.** Absorption spectra of PEDOT·CB7 PR and PEDOT·CB7 PS in ACN (a) and water (b); Fluorescence spectra in ACN of PEDOT·CB7 PR (c) and PEDOT·CB7 PS (d); Nanosecond transient absorption map of PEDOT·CB7 PR (e) and PEDOT·CB7 PS (f) in ACN ( $\lambda_{\text{ex}} = 355 \text{ nm}$ ) (the black circle shows the isosbestic points).

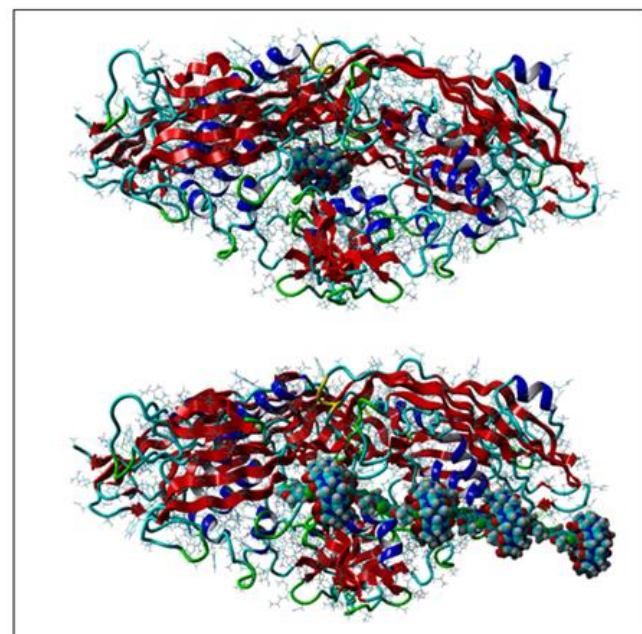
# Exploring interactions of poly(3,4-ethylenedioxythiophene/cucurbit[7]uril) polypseudorotaxane and polyrotaxanes with a biological nanopore

Nanopore resistive pulse-sensing technique and computational modeling demonstrate the strong interactions of these supramolecular compounds with a biological aerolysin nanopore.

## Electrical detection



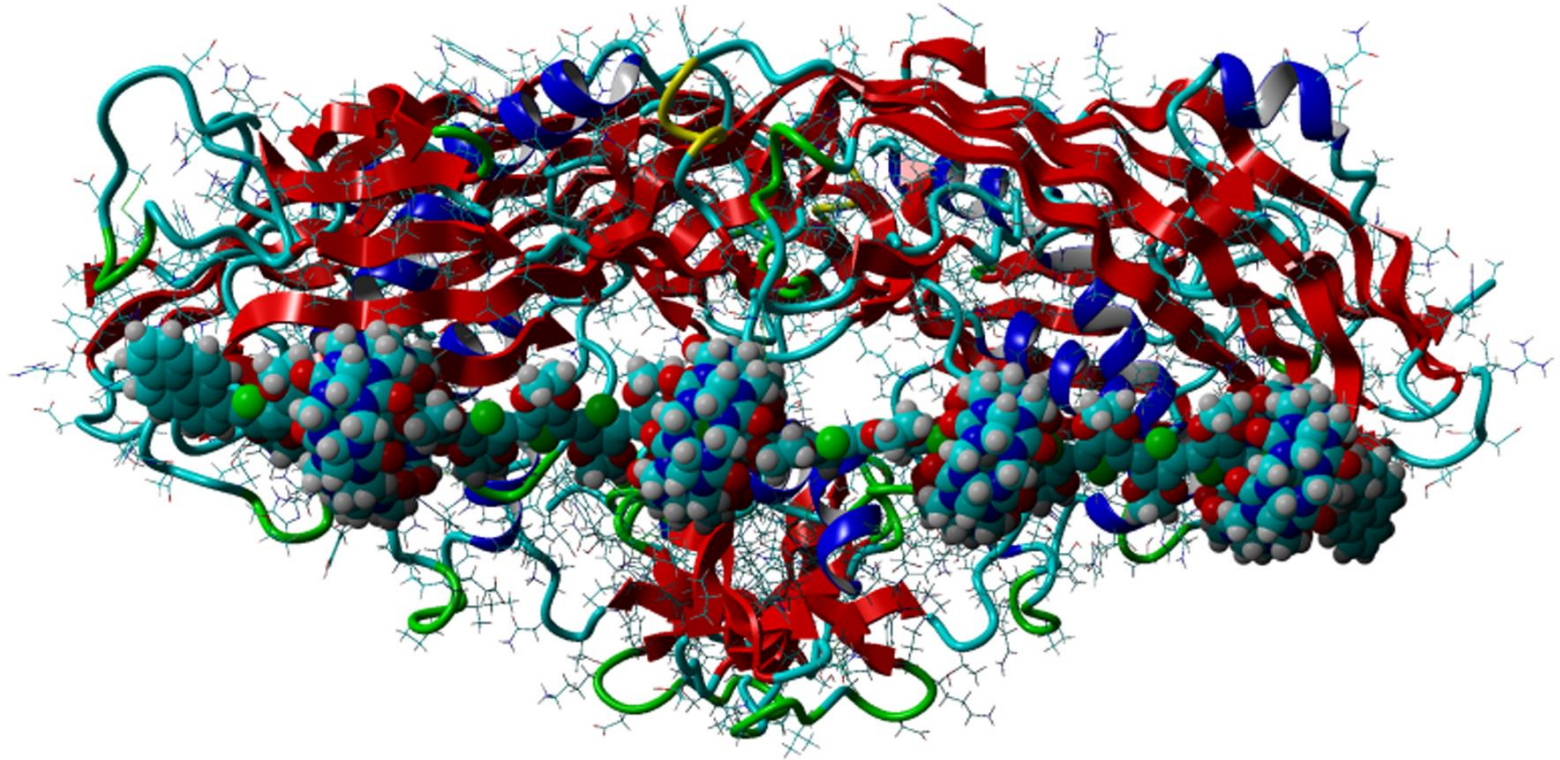
## Molecular docking

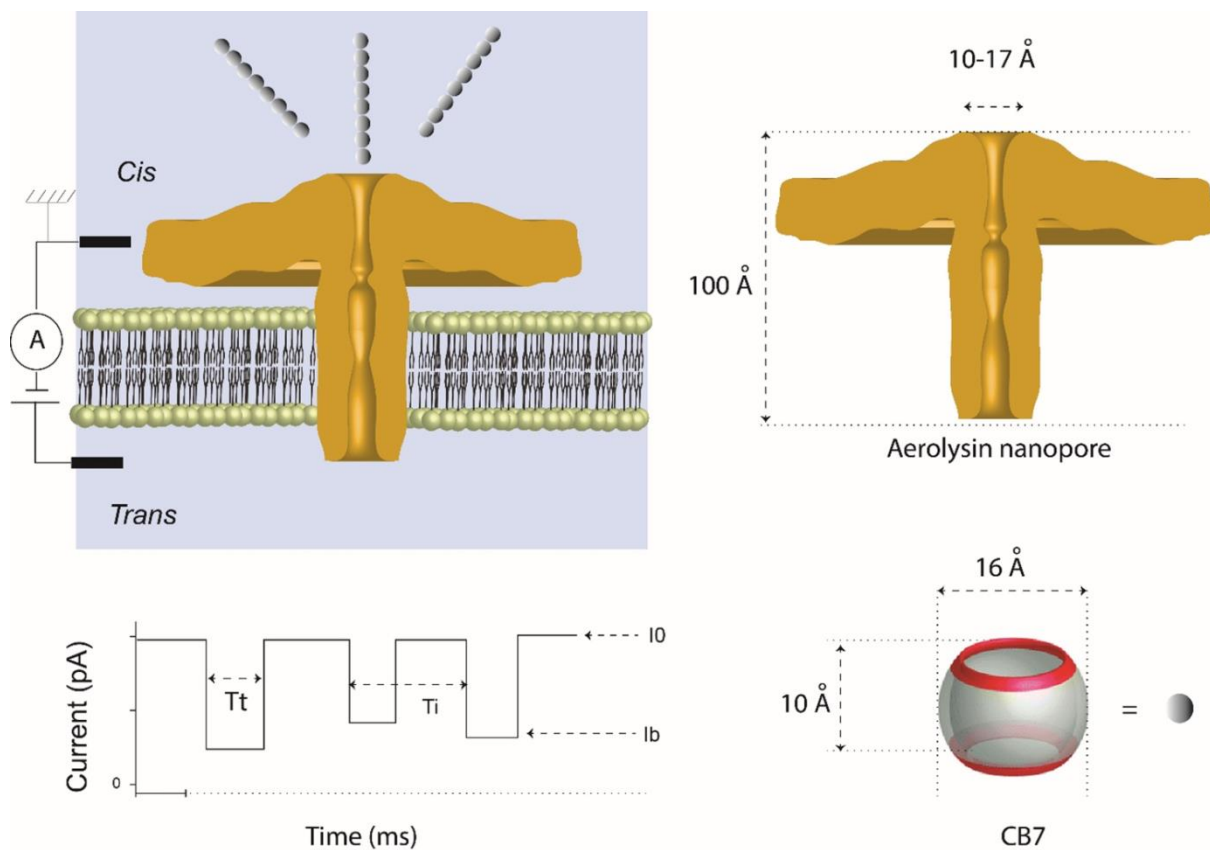


Molecular docking result: best pose of the docked complex showing the binding mode and interactions between Ael (receptor) and EDOT (up) and PEDOT·CB7-PPs (ligand) (down).



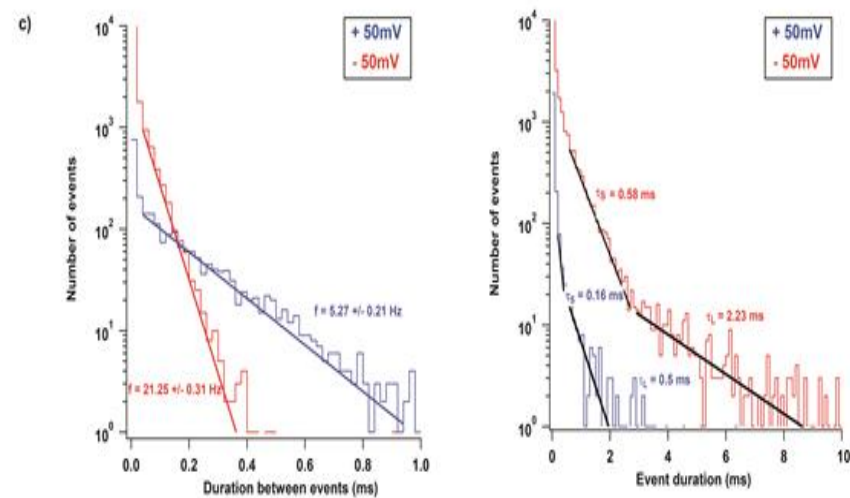
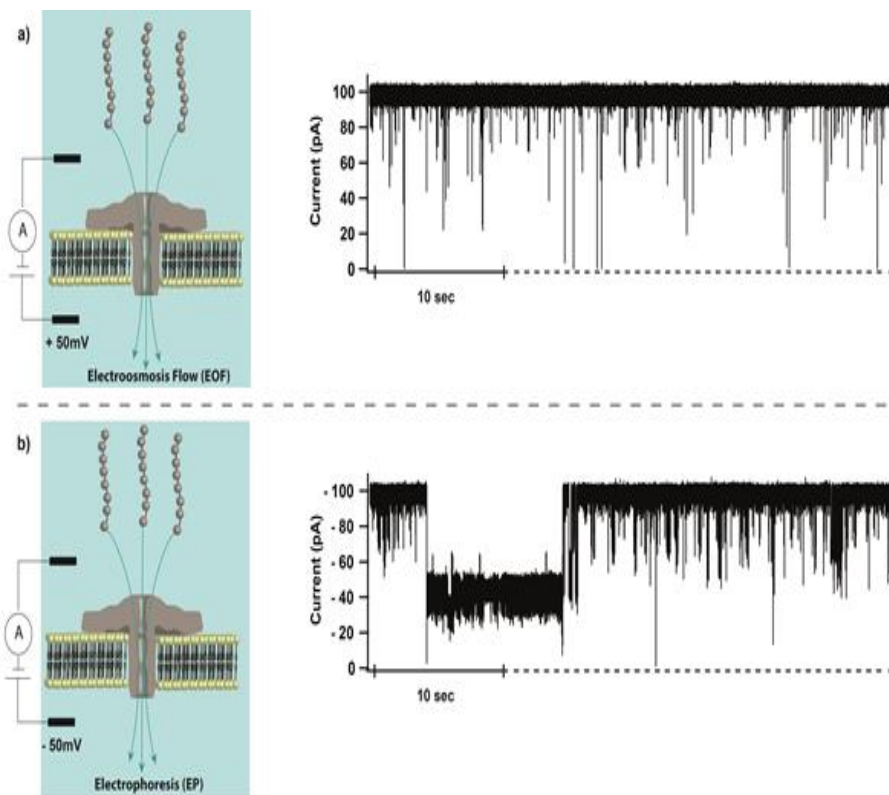
**Molecular docking result: best pose of the docked complex showing the binding mode and interactions between Ael (receptor) and PEDOT-CB7-PR (ligand)**





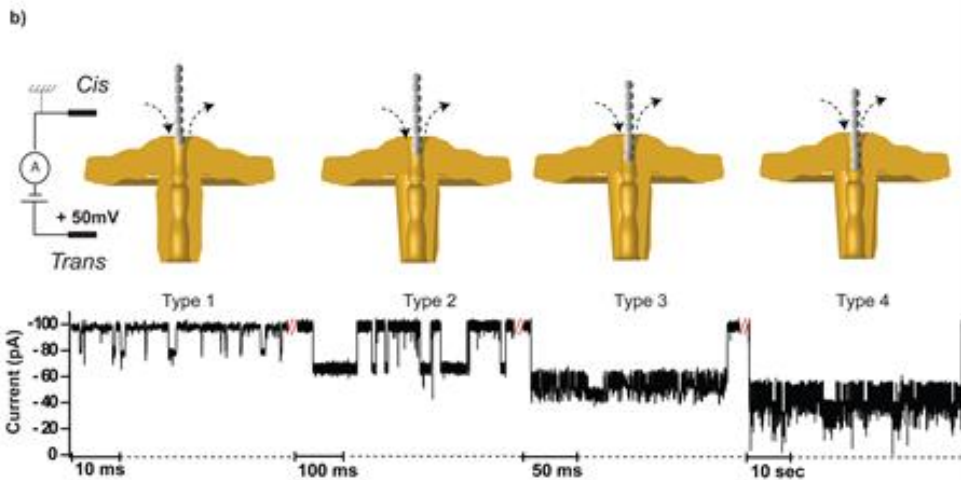
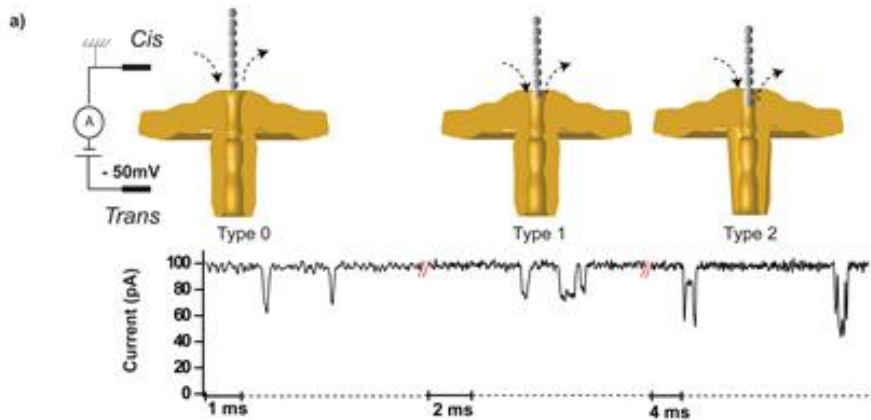
Principle of electrical detection on nanopore based single-molecule (left) and the dimensions of the Ael nanopore and the CB7 ring (right). An Ael nanopore is inserted in a planar lipid bilayer separating two compartments (*cis* and *trans*) both filled with an electrolyte. Two Ag/AgCl electrodes were used. The electrode from the *trans* compartment was used to apply a trans membrane voltage and to measure the ionic current flowing through the pore, while the electrode from the *cis* compartment is electrically grounded.

In the absence of analytes, a steady ionic current ( $I_0$ ) of mean value is flowing through the nanopore. The presence of a molecule inside the pore increases the resistance to the ion passage, which causes a partial current blockade to a lower mean current value (residual current blockade). The depth and duration of the current blockade could be associated to the size of the molecule. The initial  $I_0$  is recovered when the molecule leaves the pore.



Electrical detection of PEDOT-CB7-PPs using the Ael nanopore. Illustration of the experimental setup used for the analysis of the PEDOT-CB7-PPs added in the cis compartment in the presence of an Ael nanopore which is embedded in a lipid bilayer, arrows indicate the main driving force: Electroosmosis Flow (EOF) at positive voltage and electrophoresis (EP) at negative voltage. In all experiments cis and trans compartments were filled with 4M KCl solution buffered with 25 mM HEPES and set to pH=7.5. Portions of typical current traces recorded in the presence of 0.6 mM PEDOT-CB7-PPs under +50 mV (a) and -50 mV (b) trans applied voltages. (c) Distribution of duration between successive current blockades (events) (left) and distribution of current blockade duration (right) correspond to the full current traces recorded at +50 and -50 mV, respectively. The mean duration between successive events ( $T_i$ ) is estimated from a single exponential fit (dark solid lines) at +50 mV (blue) and -50 mV (red) (c). The  $\tau$  was estimated from a double exponential fit (dark solid lines) at +50 and -50 mV, respectively. In both representations, the left axis is in log-scale. All data were acquired at 200 kHz sampling rate and the signal was filtered at a cut-off frequency of 10 kHz.





Dependency of blockade pattern on the voltage polarity: In-zoomed portions of current traces for the interaction of PEDOT-CB7-PPs molecules with the Ael nanopore recorded at + 50 mV (a) and - 50 mV (b). At + 50 mV, almost three characteristic types of events of different shapes with durations ranging from less than 0.5 ms to 2 ms whereas at -50 mV almost four characteristic types of events of different shapes with durations ranging from ~0.1 ms to minutes are reproduced. An illustrative scheme is proposed above for each type of current. Type 0 is associated with binding events, Type 1, 2, 3 and 4 were associated to monomers (one, two, three or four, respectively) that are engaged inside the pore and that emerge from the same entry point without being translocated. At -50 mV the dominant events correspond to types 0 and 1. At +50 mV, the dominant events correspond to type 1.

**This study showed that in the trans positive voltage, almost three typical types of events occurred with durations ranging from less than 0.5 ms to a few ms (a).**

**In comparison, in the trans negative voltage, several events of different blockade duration and amplitude were identified (b).**

***This is the first time to monitor the label-free detection of PEDOT-CB7-PPs at single-molecular level by a biological Ael nanopore, which opens new perspectives.***

# Dissemination - 2022

## Published papers in ISI journal and one in proceedings online

1. A. Farcas, H. Ouldali, C. Cojocaru, M. Pastoriza-Gallego, A.-M. Resmerita, A. Oukhaled

Structural characteristics and the label-free detection of poly(3,4-ethylenedioxythiophene/ cucurbit[7]uril) pseudorotaxane at single molecule level, Nano Research 2022, online 03.10.2022, <https://doi.org/10.1007/s12274-022-4918-x>. (F.I.=10.269, Q1)

2. A.-M. Resmerita, M. Sillion, C. Cojocaru, A. Farcas

Structural and morphological characterization of a new semi-polyrotaxane architecture based on 2- hydroxypropyl- $\beta$ -cyclodextrins and polyisoprene, Reactive & Functional Polymers, 181, 105459, 2022 <https://doi.org/10.1016/j.reactfunctpolym.2022.105459> (F.I.=4.966, Q2).

3. A. Farcas, M. Damoc, M. Asandulesa, P.-H. Aubert, R. I. Tigoianu, E. L. Ursu

The straightforward approach of tuning the photoluminescence and electrical properties of encapsulated PEDOT end-capped by pyrene, Journal of Molecular Liquids, MOLLIQ-D-22-07066 (under review, F.I.=6.63, Q1)

4. M. Asandulesa, A.-M. Resmerita, A. Farcas

Electrical properties of poly(3,4-ethylenedioxythiophene) threaded by cucurbit[7]uril, Microelectronics and Nanotechnologies“ ATOM N-2022, August 22-25, Constanta-Romania, Proceedings Online OMN200-76



## International conferences

1. M. Asandulesa, A.-M. Resmerita, A. Farcas, Electrical properties of poly(3,4 ethylenedioxythiophene) threaded by cucurbit[7]uril, "Microelectronics and Nanotechnologies" ATOM N-2022, August 22-25, Constanta-Romania
2. A.-M. Resmerita, M. Balan-Porcarasu, A. Farcas, Supramolecular networks based on PEG and PEDOT cross-linked polyrotaxanes as electrical conductive materials (OMN200-55) , The 11th edition of the International Conference "Advanced Topics in Optoelectronics, Microelectronics and Nanotechnologies" ATOM N-2022, August 22-25, Constanta-Romania

## International poster

1. I. R. Tigoianu, A. Farcas  
Photophysical studies of poly(3,4 ethylenedioxythiophene/cucurbit[7]uril) polypseudorotaxane and polyrotaxane by transient absorption and time-resolved fluorescence spectroscopy, 9th International Electronic Conference on Sensors and Applications (ECSA-9), 1-15 Nov. 2022.

# Invited conferences in Germany

1. A. Farcas

Supramolecular Semi-Conducting Materials: From Synthesis to Properties and Applications

22.11.2022 Osnabruck, Germania, <https://gdch.app/event/supramolecular-semi-conducting-materials-from-synthesis-to-properties-and-applications-2022>

2. A. Farcas

Supramolecular Semiconductor Materials for Organic Electronics, 25.11. 2022, Bremen University, Germany

## Other

1. A. Farcas - Program Committee at the 11th edition of the International Conference "Advanced Topics in Optoelectronics, Microelectronics and Nanotechnologies" ATOM N-2022, August 22-25, Constanta-Romania
2. A. Farcas - Program Committee and KEYNOTE SPEAKER at the International Summit on Power and Energy Engineering (ISPEE 2023), 12-14 Jun 2023, Paris France
3. A. Farcas - The board member in the Journal of Composites and Biodegradable Polymers